

Resonant inelastic soft x-ray scattering of Be chalcogenides

D. Eich, O. Fuchs, U. Groh, L. Weinhardt, R. Fink, and E. Umbach
Experimentelle Physik II, Universität Würzburg, Am Hubland, 97074 Würzburg, Germany

C. Heske*
Department of Chemistry, University of Nevada, Las Vegas, Nevada 89154-4003, USA

A. Fleszar and W. Hanke
Theoretische Physik I, Universität Würzburg, Am Hubland, 97074 Würzburg, Germany

E. K. U. Gross
Theoretische Physik I, Universität Würzburg, Am Hubland, 97074 Würzburg, Germany
and Institut für Theoretische Physik, Freie Universität Berlin, Arnimallee 14, 14195 Berlin, Germany

C. Bostedt, T. v. Buuren, N. Franco, and L. J. Terminello
Lawrence Livermore National Laboratory, University of California, Livermore, California 94551, USA

M. Keim, G. Reuscher, H. Lugauer, and A. Waag[†]
Experimentelle Physik III, Universität Würzburg, Am Hubland, 97074 Würzburg, Germany
 (Received 6 February 2006; published 30 March 2006)

The bulk electronic band structures of BeTe and BeSe have been studied by resonant inelastic soft x-ray scattering (RIXS) at the Be 1s edge. We derive direct and indirect bulk band gaps and observe the coexistence of core excitons and momentum conservation. A quantitative analysis of the coherent spectral fraction gives insight into the femtosecond time scale of the relevant dephasing processes. Experimental results agree very well with calculations based on the Kramers-Heisenberg and density-functional theories.

DOI: [10.1103/PhysRevB.73.115212](https://doi.org/10.1103/PhysRevB.73.115212)

PACS number(s): 71.20.Nr, 71.15.Mb, 78.70.Ck, 78.70.En

I. INTRODUCTION

Studying the electronic band structure of solids has been one of the central tasks of surface and solid state science for the last 30 years, and a vast variety of band structures has been determined by combining angle-resolved photoelectron spectroscopy (ARPES) with suitable theoretical calculations. However, ARPES is limited to systems in which well-defined and conductive surfaces can be prepared in an ultrahigh vacuum (UHV) environment. Thus, for many materials (such as the Be chalcogenides), very little is known about their electronic band structure, since they exhibit large band gaps and poor conductivity, or since no simple surface preparation routines exist (and a proper UHV transfer^{1,2} is difficult or impossible).

With the advent of high-brilliance third-generation synchrotron sources, a new approach to study the bulk band structure has been established, namely to utilize resonant inelastic x-ray scattering (RIXS) in the soft x-ray regime.³ In RIXS, an electronic Raman scattering process is used to select specific excitations of valence electrons into unoccupied conduction band states.⁴ In an alternative (but synonymous) description, a core electron is resonantly excited into an unoccupied state at a certain \mathbf{k} value, and the resonant fluorescence decay of a valence electron with the same \mathbf{k} value into the core hole is detected. The observed RIXS spectrum hence contains momentum-resolved information about the occupied and unoccupied electronic states, which can be analyzed on the basis of the Kramers-Heisenberg formalism. Because

the information depth is typically on the order of a few hundred nanometers, the study of systems with poorly defined surfaces or protective cap layers becomes possible.

Since the first resonant x-ray emission spectra using synchrotron radiation,⁵ a vivid discussion of resonance effects in RIXS has been conducted.⁵⁻¹⁴ Today it is widely accepted that band structure effects can be readily observed, and that this finding is true also for material systems with core excitons.^{8,10,11} It is the purpose of this paper to demonstrate that RIXS indeed describes the band structure of Be-chalcogenides excellently and that the experimental spectra agree very well with *ab initio* calculations based on band structures derived with various approximations to the density-functional theory. Furthermore, information about the dephasing processes on a fs time scale can be gained.

The Be chalcogenides BeSe and BeTe are interesting materials among the class of II-VI semiconductors due to their strongly covalent nature and hence relatively high mechanical hardness. It is hence favorable to include Be-chalcogenides into optoelectronic II-VI semiconductor devices, e.g., laser diodes based on ZnSe, in order to improve the lifetime of the device.¹⁵ Unlike all other II-VI semiconductors, BeTe and BeSe possess an indirect band gap, the size of which is experimentally not very well established. VUV ellipsometry experiments give a *direct* band gap of 4.2 eV (5.55 eV) for BeTe (BeSe),¹⁶ while optical reflection experiments derive 4.35 eV (5.65 eV).¹⁷ The *indirect* band gap of BeTe is 2.8 eV (reflection) or 2.7 eV (absorption), while no experimental data for BeSe exists.¹⁸ As will be

discussed below, such band gap information, both for the indirect band gap as well as for direct band gaps at selected points in the Brillouin zone, can be readily derived from the experimental RIXS spectra.

II. EXPERIMENT AND THEORY

The experimental RIXS and fluorescence yield x-ray absorption (XAS) spectra were recorded at beamline 8.0 of the Advanced Light Source, Lawrence Berkeley Laboratory. The combined energy resolution of beamline and spectrometer was chosen to be better than 0.25 eV. Thin epitaxial films of BeTe (300 nm) and BeSe (800 nm) were grown with molecular beam epitaxy on GaAs(100) substrates. In the case of BeTe, an additional ZnSe buffer layer (50 nm) and a ZnSe cap layer (20 nm) were included to enhance the crystal quality and to prevent oxidation after removal from UHV, respectively. Note that the ability to probe the band structure through a protective cap layer is a unique feature of RIXS studies. Theoretical RIXS spectra of BeTe and BeSe were calculated on the basis of the Kramers-Heisenberg and density functional theories.¹⁹ The exchange-correlation functional was given either by the local-density approximation (LDA) or the exact-exchange (EXX) method.²⁰ The calculations utilized pseudopotentials which were generated in accordance with the exchange-correlation functional (LDA-PP and EXX-PP, resp.).²¹ In these pseudopotential calculations, the Be 1s core state was modeled as a localized Gaussian of *s*-symmetry placed at the beryllium sites. An additional LDA calculation was conducted by taking the Be 1s states explicitly into account (LDA-all). For comparison with experiment, all calculations were adjusted by energy offsets for excitation and emission (constant for each material), respectively. These offsets were chosen such that the best agreement between theoretical and experimental spectra was obtained. This procedure leads to values for the indirect band gap of 2.7 eV (3.6 eV) for BeTe (BeSe), which is only 0.1 eV larger (smaller) than the values from a quasiparticle calculation²² using the GW approximation.²³

III. RESULTS AND DISCUSSION

The complete set of RIXS spectra as a function of excitation energy is shown in Fig. 1 for BeTe (left) and BeSe (right). In the spectra with lowest excitation energy, “E” denotes the elastic scattering channel (i.e., the Rayleigh line), which shifts to higher emission energy as a function of excitation energy (see right ordinates). For BeSe, below the absorption edge (114.9 eV), the peak labeled “R” follows this shift with a fixed energy separation. It is associated with a constant (Raman-like) loss feature, which we attribute to the excitation of a valence electron into the conduction band with an energy of 6.9 ± 0.15 eV. Due to momentum conservation and a negligible momentum transfer of the soft x-ray photons, this excitation must be a direct transition. Two points in *k*-space are particularly suited for this transition, first the L point, for which we calculate the largest theoretical matrix element and which corresponds to a band gap of 6.6 eV,²² and second the X point, for which the virtual inter-

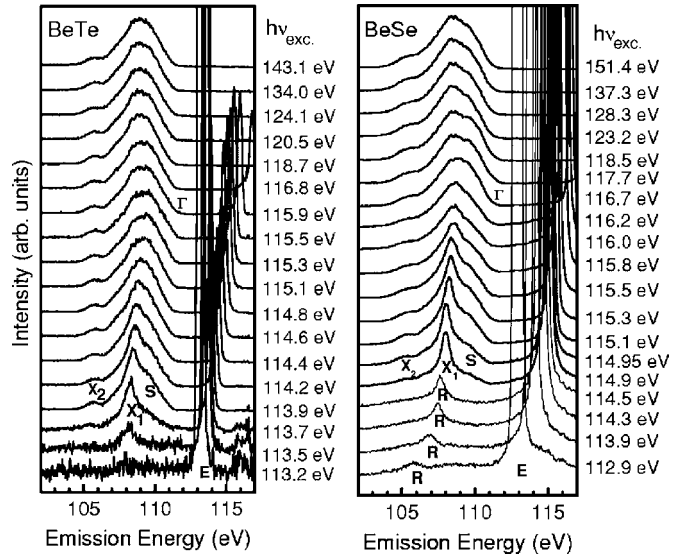


FIG. 1. Resonant inelastic soft x-ray scattering (RIXS) spectra of BeTe (left) and BeSe (right). The excitation photon energy for each spectrum is given at the right ordinate of each graph. The elastic scattering channel (E), major valence band emissions at high-symmetry points in *k*-space (X_1, X_2, Γ), Raman-type dispersive features below the absorption edge (R), and a shoulder (S) are discussed in the text. The intensity of each spectrum was arbitrarily rescaled for better viewing.

mediate state is closest to a real state (i.e., the conduction band minimum), corresponding to a band gap of 6.5 eV.²² No “R” features are observed for our BeTe sample, perhaps due to signal attenuation in the ZnSe cap layer.

The spectra observed at the BeTe and BeSe absorption onsets (above 113.5 eV and 114.9 eV, resp.) stem from RIXS processes involving an excitation into the conduction band minimum, i.e., at the X point. Consequently, the observed spectral features (labeled X_1 and X_2) correspond to the occupied electronic states at the X point. Furthermore, a high-energy shoulder (S) is observed, which we interpret as arising from scattering processes (e.g., electron-phonon scattering) involving states near the valence band maximum (VBM) at the Γ point. Such scattering processes “destroy” the momentum information of some fraction of the RIXS spectrum which is hence considered to be “incoherent.” In order to obtain the desired coherent fraction, we have followed the approach described in Ref. 11: a maximal fraction of a spectrum with an excitation energy well above threshold is taken as an “incoherent” reference spectrum and is subtracted from each RIXS spectrum (with the apparent boundary condition that no negative intensities occur).

A comparison of the coherent fraction of the near-threshold RIXS spectra (thin solid lines with noise) with theoretical spectra is shown in Figs. 2 and 3. In Fig. 2, the theoretical spectra (smooth lines) were derived by EXX-PP for BeTe and LDA-all for BeSe, which gave best agreement with the experimental data, as will be discussed below. All energies are given with respect to the VBM. The signal-to-noise ratio of the experimental coherent fraction, by construction, is small for spectra excited several eV above

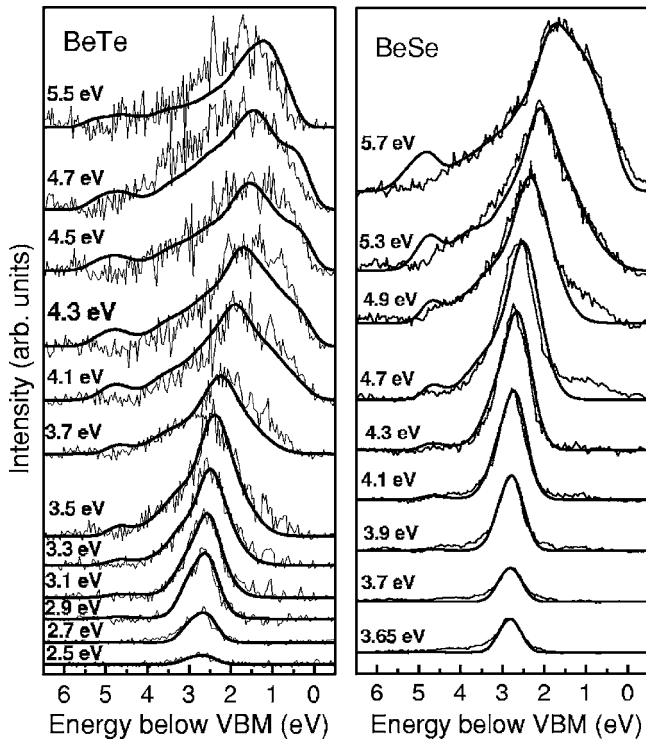


FIG. 2. Coherent fraction of the spectra in Fig. 1 (left: BeTe; right: BeSe) and best theoretical spectra (noise-free curves) computed using the local density approximation (LDA) with a direct description of the core hole for BeSe, and using an exact-exchange approach for BeTe. As the abscissa, the binding energy below the valence band maximum (VBM) is used, and the denoted excitation energies are referenced to the VBM.

threshold. For BeTe, it is further reduced due to the signal attenuation by the ZnSe cap layer. Nevertheless, the overall agreement between experiment and theory is remarkably good, the largest deviations occurring near the bottom of the valence band, which leads us to conclude that additional scattering processes might play an important role in that range. Furthermore, a few of the BeSe spectra exhibit an additional shoulder at the VBM, which we ascribe to shortcomings in the employed subtraction method.

We observe that different exchange-correlation approximations were found to be best suited to describe the experimental spectra for the two different materials. Figure 3 shows an exemplary comparison of the different approximations for selected excitation energies (EXX-PP, dashed; LDA-PP, dotted; LDA-all, solid). Note that the comparison was limited to a few cases for visual clarity only; these are representative of the overall trends. In the case of BeSe, the best overall agreement was found for the two LDA approaches (after adjusting the theoretical band gaps to 3.6 eV), with somewhat better results being obtained by taking the Be $1s$ state explicitly into account (LDA-all). Note, however, that the differences between LDA-PP and LDA-all are very small. This fact suggests that the fulfillment of optical-transition selection rules—as satisfied by a model core state, e.g., an s -type Gaussian—is more important in RIXS calculations than the exact description of the core

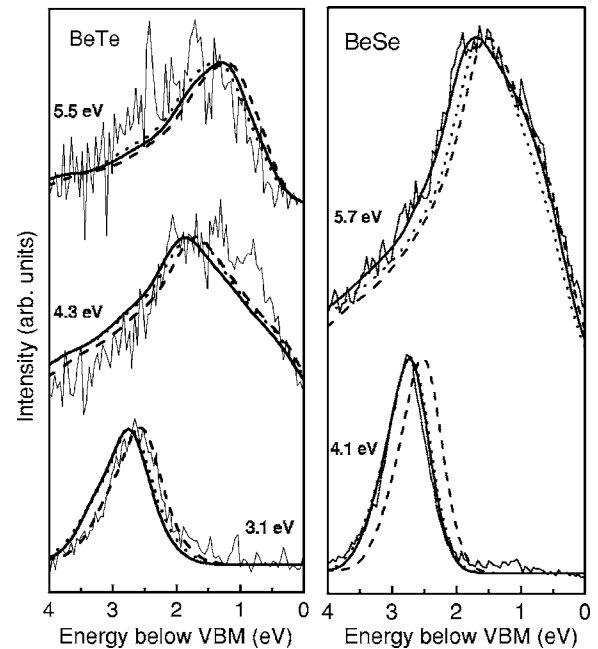


FIG. 3. Coherent fraction of the spectra in Fig. 1 (left: BeTe; right: BeSe) at selected excitation energies and theoretical spectra (noise-free curves) computed using the local density approximation (LDA) with a direct description of the core hole (solid line), using an exact-exchange approach (dashed line), and using LDA with a pseudopotential description of the Be $1s$ states (dotted line). As an abscissa, the binding energy below the valence band maximum (VBM) is used, and the denoted excitation energies are referenced to the VBM.

state. The improved description by LDA is a direct consequence of the fact that in EXX a too narrow band width is determined.²⁰ In the case of BeTe, the significantly worse signal to noise ratio of the experimental data makes a distinction between the different approximations more difficult. The best agreement is found for the EXX approach and an indirect band gap of 2.7 eV, while a reduction of the band gap to 2.5 eV gives a slightly poorer, but still reasonable agreement for the LDA approaches as well.

At one point in the development of RIXS for band structure determinations, it was strongly debated whether the existence of a core exciton would allow the collection of momentum-resolved RIXS spectra at all.^{8–11} As shown in Fig. 4 for BeTe and BeSe, the answer clearly is “yes.” Figure 4 presents nonresonant x-ray emission spectra (thus abbreviated “XES” rather than “RIXS”), which were recorded at the so-called “second threshold”²⁴ (118.9 eV for BeTe and 121.8 eV for BeSe, corresponding to approx. 5.4 eV and 6.9 eV above the absorption onset, resp.). At the “second threshold,” the majority of excitations and de-excitations occurs without retaining the momentum information (incoherent emission). However, a small number of processes leads to a resonant scattering via a core-excitonic state *together* with the excitation of a second electron (a kind of shake up process). In other words, a Be $1s$ core electron is excited into the core-excitonic state *and* simultaneously an additional valence electron is excited from the valence band into the con-

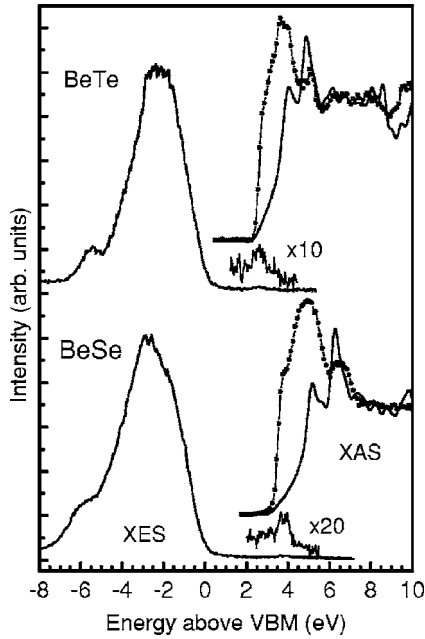


FIG. 4. Combined emission (XES) and experimental (solid lines with data points) as well as theoretical (thick solid lines) absorption (XAS) spectra of BeTe (top) and BeSe (bottom). All spectra are shown on a joint energy scale with respect to the valence band maximum (VBM). The XES spectra were recorded at the “second threshold” (BeTe: $h\nu=118.9$ eV, BeSe: $h\nu=121.8$ eV). The emission from core excitons is shown on enlarged scales.

duction band (or vice versa), followed by the (coherent) de-excitation process of the core-excitonic state alone. The latter can be observed at a fixed photon energy a few eV above that of the VBM, as shown in Fig. 4 on a magnified scale. Note, that for both involved electrons k conservation is required, but the shake up process may occur at a different k value as compared to the core exciton which is expected to occur at the X point.

The energy position of the core exciton in BeTe and BeSe is 2.60.2 eV and 3.8 ± 0.2 eV above the valence band maximum, respectively. These values agree well with a separate determination based on the RIXS spectra in Fig. 1; comparing the valence band maximum position with the Rayleigh line at the absorption onset, one derives indirect core-excitonic band gaps of 2.5 ± 0.15 eV for BeTe and 3.8 ± 0.15 eV for BeSe. The positions of the core excitons coincide nicely with the onset of absorption in the experimental XAS spectra (Fig. 4, solid dots) within the limits of spectral resolution, as expected. The smooth solid XAS spectra without dots were obtained from the band structure calculations, taking matrix elements into account, but—as is the case in one-particle theories—neglecting core hole effects. While the theoretical spectra give a reasonable overall agreement with experiment after alignment of the energy axis to match the absorption edge onset, we find significant deviations directly above the onset, in particular for the curvature of the leading edge. This can be readily explained by the presence of the core exciton states. Their position above the VBM is in good agreement with the indirect band gaps discussed above.

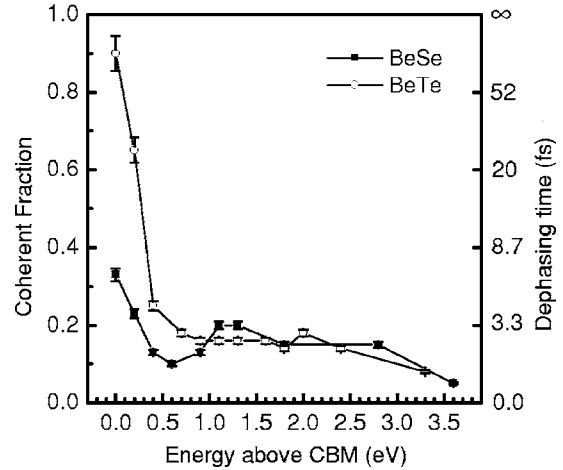


FIG. 5. Coherent fraction (left) and dephasing time (right) of the RIXS spectra of BeTe and BeSe as a function of excitation energy above the conduction band minimum (CBM). Error bars are based on the uncertainty in determining the correct coherent fraction by the subtraction method described in the text.

As mentioned, the RIXS spectra also allow the determination of *direct* band gaps. The gap at the X point is derived by using the above-determined indirect gap and adding the energetic difference between emission from the upper occupied states at the X and Γ point. This procedure derives direct gaps at the X point of 6.80 ± 0.15 eV for BeSe and 5.40 ± 0.15 eV for BeTe, the former being close and the latter being identical to the GW values in Refs. 20 and 22 (6.5 and 5.4 eV, respectively). For BeSe, the direct gap at the X point agrees very well with the separation between the Raman-like loss feature (R) and the elastic line (6.9 ± 0.15 eV), as discussed above in conjunction with Fig. 1. The direct gap at the Γ point is determined as the excitation energy (with respect to the VBM) of the spectrum with strongest spectral contribution from the VBM, leading to values of 4.5 ± 0.2 eV for BeTe and 5.7 ± 0.2 eV for BeSe. These values exceed the GW results by about 0.2 eV in both cases and the previously obtained optical data by ~ 0.2 and ~ 0.1 eV, respectively.

The coherent fraction of each RIXS spectrum can be utilized to extract temporal information about the dephasing processes.³ Figure 5 presents the coherent fractions (left ordinate) for BeTe (open symbols) and BeSe (filled symbols) as a function of excitation energy, plotted as energy above the conduction band minimum. The error bars were determined empirically from the subtraction routine discussed above. First, we observe that the coherent fraction decreases rapidly with increasing excitation energy, which is due to the fact that the probability for electron-phonon scattering processes involving the *emission* or *absorption* of a phonon increases when moving “up” from the conduction band minimum. Secondly, the coherent fraction near threshold is significantly larger for BeTe than for BeSe, which we can possibly ascribe to the fact that the (Fröhlich) coupling between electrons and phonons is expected to be stronger in BeSe than in BeTe.²⁵ The derived coherent fractions from Fig. 5 can directly be converted into dephasing times with a “core hole clock” formalism.²⁶ If the core hole decays before

phonon scattering takes place, the x-ray absorption/emission process can be considered as a coherent (one-step) inelastic scattering process; if the phonon scattering time is shorter the coherence between x-ray excitation and emission process and hence k conservation is destroyed. Based on the Be $1s$ lifetime of ≈ 13 fs,²⁷ we can compute²⁶ the dephasing time τ as a function of excitation energy (right ordinate of Fig. 5). Note that the Be $1s$ core hole lifetime is expected to be very similar for Be metal and the semiconductors probed here, since it is primarily determined by the time scale of the Auger decay (even if, like in the present case, the radiative decay channel is investigated). We find that τ can be as long as 120 fs (6 fs) for BeTe (BeSe) directly at threshold, and diminishes to less than 3 fs above the threshold. This demonstrates the capability of RIXS to study the dynamics of electron-phonon coupling on the femtosecond time scale.

IV. SUMMARY

We find that the coherent fraction of resonant soft x-ray scattering spectra of BeTe and BeSe agrees very well with theoretically calculated spectra based on the Kramers-Heisenberg formalism and a band structure derived from density functional theory. From the experimental data alone

we determine the band gaps of BeTe and BeSe, respectively [BeTe: indirect: 2.6 eV, direct: 5.4 eV (X-point) and 4.5 eV (Γ -point), BeSe: indirect: 3.8 eV, direct: 6.8 eV (X-point) and 5.7 eV (Γ -point)], in good agreement with corresponding theoretical values. By exciting emission spectra above the second threshold, we find direct evidence for the presence of core excitons and their fluorescent decay in these systems. Furthermore, we can derive information about the relevant time scales for dephasing processes governed by electron-phonon scattering as a function of excitation energy. At threshold they are significantly larger for BeTe than for BeSe and range from 120 fs (BeTe; at threshold) to 3 fs (both; markedly above threshold). In combination, these results demonstrate the versatility of RIXS to study electronic and dynamic aspects of material systems which, for a variety of reasons (including the presence of a protective cap layer), are not accessible with the conventional band structure method of angle-resolved photoelectron spectroscopy.

ACKNOWLEDGMENTS

We gratefully acknowledge the technical support of the ALS staff as well as funding by the DFG through SFB 410, TP B3, B4, and A3. The calculations were performed at the ZAM Jülich.

*Author to whom correspondence should be addressed. Electronic address: heske@unlv.nevada.edu; Tel.: (702) 895 2694; Fax: (702) 895 4072.

[†]Present address: Institut für Halbleitertechnik, TU Braunschweig, 38106 Braunschweig, Germany.

¹M. Nagelstraßer, H. Dröge, H.-P. Steinrück, F. Fischer, T. Litz, A. Waag, G. Landwehr, A. Fleszar, and W. Hanke, Phys. Rev. B **58**, 10394 (1998), and references therein.

²V. Wagner, J. Wagner, S. Gundel, L. Hansen, and J. Geurts, Phys. Rev. Lett. **89**, 166103 (2002).

³S. Eisebitt and W. Eberhardt, J. Electron Spectrosc. Relat. Phenom. **110-111**, 335 (2000), and references therein.

⁴Note that, for our energies and materials, the photon momentum (0.045 \AA^{-1}) is less than 2% of the width of the Brillouin zone along the X- Γ -X direction (2.4 \AA^{-1}) and can hence be neglected.

⁵J.-E. Rubensson, N. Wassdahl, G. Bray, J. Rindstedt, R. Nyholm, S. Cramm, N. Mårtensson, and J. Nordgren, Phys. Rev. Lett. **60**, 1759 (1988); J.-E. Rubensson, D. Mueller, R. Shuker, D. L. Ederer, C. H. Zhang, J. Jia, and T. A. Callcott, *ibid.* **64**, 1047 (1990).

⁶Y. Ma, N. Wassdahl, P. Skytt, J. Guo, J. Nordgren, P. D. Johnson, J.-E. Rubensson, T. Boske, W. Eberhardt, and S. D. Kevan, Phys. Rev. Lett. **69**, 2598 (1992); **49**, 5799 (1994).

⁷K. E. Miyano, D. L. Ederer, T. A. Callcott, W. L. O'Brien, J. J. Jia, L. Zhou, Q.-Y. Dong, Y. Ma, J. C. Woicik, and D. R. Mueller, Phys. Rev. B **48**, 1918 (1993).

⁸J. A. Carlisle, E. L. Shirley, E. A. Hudson, L. J. Terminello, T. A. Callcott, J. J. Jia, D. L. Ederer, R. C. C. Perera, and F. J. Himpsel, Phys. Rev. Lett. **74**, 1234 (1995); **59**, 7433 (1999).

⁹M. van Veenendaal and P. Carra, Phys. Rev. Lett. **78**, 2839 (1997).

¹⁰E. L. Shirley, Phys. Rev. Lett. **80**, 794 (1998).

¹¹J. Lüning, J.-E. Rubensson, C. Ellmers, S. Eisebitt, and W. Eberhardt, Phys. Rev. B **56**, 13147 (1997).

¹²A. Agui, S. Shin, M. Fujisawa, Y. Tezuka, T. Ishii, Y. Muramatsu, O. Mishima, and K. Era, Phys. Rev. B **55**, 2073 (1997).

¹³L.-C. Duda, J. Downes, C. McGuinness, T. Schmitt, A. Augustsson, K. E. Smith, G. Dhalenne, and A. Revcolevschi, Phys. Rev. B **61**, 4186 (2000).

¹⁴A. V. Sokolov, L. D. Finkelstein, E. Z. Kurmaev, S. Shin, P. F. Karimov, N. A. Skorikov, and A. V. Postnikov, J. Electron Spectrosc. Relat. Phenom. **137-140**, 591 (2004).

¹⁵A. Waag, Th. Litz, F. Fischer, H.-J. Lugauer, T. Baron, K. Schüll, U. Zehnder, T. Gerhard, U. Lunz, M. Keim, G. Reuscher, and G. Landwehr, J. Cryst. Growth **184/185**, 1 (1998).

¹⁶K. Wilmers, T. Wethkamp, N. Esser, C. Cobet, W. Richter, V. Wagner, A. Waag, H. Lugauer, F. Fischer, T. Gerhard, M. Keim, and M. Cardona, Phys. Status Solidi B **215**, 15 (1999).

¹⁷F. Fischer, doctoral thesis, Würzburg (1998).

¹⁸*Landoldt-Börnstein: II-VI and I-VII Compounds* (Springer, Berlin, Heidelberg, 1999), Vol. 41B.

¹⁹P. Hohenberg and W. Kohn, Phys. Rev. **136**, B864 (1965); W. Kohn and L. J. Sham, Phys. Rev. **140**, A1133 (1965).

²⁰A. Fleszar, Phys. Rev. B **64**, 245204 (2001).

²¹M. Moukara, M. Städele, J. A. Majewski, P. Vogl, and A. Görling, J. Phys.: Condens. Matter **12**, 6783 (2000).

²²A. Fleszar and W. Hanke, Phys. Rev. B **62**, 2466 (2000).

²³For a review see, G. Onida, L. Reinig, and A. Rubio, Rev. Mod. Phys. **74**, 601 (2002).

- ²⁴W. L. O'Brien, J. Jia, Q.-Y. Dong, T. A. Callcott, K. E. Miyano, D. L. Ederer, D. R. Mueller, and C.-C. Kao, *Phys. Rev. Lett.* **70**, 238 (1993).
- ²⁵D. Eich, doctoral thesis, Würzburg (2000).
- ²⁶O. Björneholm, A. Nilsson, A. Sandell, B. Hernäs, and N. Mårtensson, *Phys. Rev. Lett.* **68**, 1892 (1992).
- ²⁷J. N. Andersen, T. Balasubramanian, C.-O. Almbladh, L. I. Johansson, and R. Nyholm, *Phys. Rev. Lett.* **86**, 4398 (2001).